Chemosphere xxx (2013) xxx–xxx

Contents lists available at SciVerse ScienceDirect

Chemosphere

journal homepage: www.elsevier.com/locate/chemosphere

Atmospheric partitioning and the air–water exchange of polycyclic aromatic hydrocarbons in a large shallow Chinese lake (Lake Chaohu)

Ning Qin, Wei He, Xiang-Zhen Kong, Wen-Xiu Liu, Qi-Shuang He, Bin Yang, Hui-Ling Ouyang, Qing-Mei Wang, Fu-Liu Xu *

MOE Laboratory for Earth Surface Processes, College of Urban & Environmental Sciences, Peking University, Beijing 100871, China

HIGHLIGHTS

- Levels and distribution of atmospheric and water PAHs were studied in Lake Chaohu.
- The monthly diffusive air–water exchange flux were estimated by a two-film model.
- PAH16 levels in atmosphere and water were significantly correlated with temperature.
- Significant correlations between gas-particle partition and log P_L^O and Log K_{oa}.
- PAH levels in water and gas were the most important factors for air–water exchange.

ARTICLE INFO

Article history:
Received 20 November 2012
Received in revised form 16 May 2013
Accepted 20 May 2013
Available online xxxx

Keywords:
Polycyclic aromatic hydrocarbons
Atmospheric partitioning
Air–water exchange
Uncertainty analysis
Lake Chaohu

ABSTRACT

The residual levels of polycyclic aromatic hydrocarbons (PAHs) in the atmosphere and in dissolved phase from Lake Chaohu were measured by (GC–MS). The composition and seasonal variation were investigated. The diffusive air–water exchange flux was estimated by a two-film model, and the uncertainty in the flux calculations and the sensitivity of the parameters were evaluated. The following results were obtained: (1) the average residual levels of all PAHs (PAH16) in the atmosphere from Lake Chaohu were 60.85 ± 46.17 ng m^{-3} in the gaseous phase and 14.32 ± 23.82 ng m^{-3} in the particulate phase. The dissolved PAH16 level was 173.46 ± 132.89 ng L^{-1}. (2) The seasonal variation of average PAH16 contents ranged from 43.09 ± 33.20 ng m^{-3} (summer) to 137.47 ± 41.69 ng m^{-3} (winter) in gaseous phase, from 6.62 ± 2.72 ng m^{-3} (summer) to 56.13 ± 22.99 ng m^{-3} (winter) in particulate phase, and 142.68 ± 74.68 ng L^{-1} (winter) to 360.00 ± 176.60 ng L^{-1} (summer) in water samples. Obvious seasonal trends of PAH16 concentrations were found in the atmosphere and water. The values of PAH16 for both the atmosphere and the water were significantly correlated with temperature. (3) The monthly diffusive air–water exchange flux of total PAH16 ranged from -1.77×10^4 ng m^{-2} d^{-1} to 1.11×10^5 ng m^{-2} d^{-1}, with an average value of 3.45×10^4 ng m^{-2} d^{-1}. (4) The results of a Monte Carlo simulation showed that the monthly average PAH fluxes ranged from -3.4×10^3 ng m^{-2} d^{-1} to 1.6×10^4 ng m^{-2} d^{-1} throughout the year, and the uncertainties for individual PAHs were compared. (5) According to the sensitivity analysis, the concentrations of dissolved and gaseous phase PAHs were the two most important factors affecting the results of the flux calculations.

1. Introduction

Polycyclic aromatic hydrocarbons (PAHs) are a group of compounds composed of two or more fused aromatic rings (Menzie et al., 1992). PAHs occur in the environment as complex mixtures of many components (Petry et al., 1996). They mainly originate from coal combustion, vehicle emissions, the coking industry, and the burning of biomass (Rogge et al., 1993; Kavouras et al., 2001; Xu et al., 2006). They have been a topic of concern because of their potentially toxic, mutagenic, and carcinogenic properties (Khalili et al., 1995; Fernandes et al., 1997; Larsen and Baker, 2003). Therefore, 16 PAHs are included in the priority pollutants list of the US EPA. During last decades, the PAH emissions in China have been increasing greatly with the rapid population growth and economic development (Xu et al., 2006; Zhang et al., 2007b). China is suffering from severe contamination of PAHs from various sources, which poses a serious threat to ecosystems and human health (Xu et al., 2011, 2013). The emissions of 16 priority PAHs in China was estimated as 25 300 tons in 2003, and among various emission sources, biomass burning, domestic coal combustion, and coking industry contributed 60%, 20%, and 16% of the total

* Corresponding author. Tel.: +86 10 62751177; fax: +86 10 62751187.
E-mail address: xufl@urban.pku.edu.cn (F.-L. Xu).

0045-6535/$ - see front matter © 2013 Elsevier Ltd. All rights reserved.
http://dx.doi.org/10.1016/j.chemosphere.2013.05.038

emission, respectively (Xu et al., 2006). The higher PAHs emission density was found in the southeastern provinces, while the higher PAHs emission intensity and population-normalized emission were found in western and northern China (Xu et al., 2006).

A body of water can act either as a sink (Lohmann et al., 2006) or as a source (Zhang et al., 2007a) for PAHs in the environment. The atmosphere plays an important role in PAH contamination of water bodies (Simonich and Hites, 1995; Simcik et al., 1999). Wet deposition, dry deposition, and gas exchange across the air–water interface are the three major transport pathways for atmospheric inputs of organic pollutants into the Great Lakes (Franz et al., 1998). Unlike wet and dry deposition, gas exchange is a "two-way street" (McConnell et al., 1993). Therefore, gas exchange appears to be an important process that controls the concentrations and residence times of PAHs in natural water bodies (Pandit et al., 2006). Air–water exchange is a complex process controlled by many factors. In recent decades, much work has been done on the estimation of the air–water exchange of POPs (Nelson et al., 1998; Wania et al., 1998; Totten et al., 2001; Tsapakis et al., 2006). Two-film models were usually employed to estimate the exchange flux quantitatively. However, model uncertainty and the impact of parameters were seldom discussed.

Lake Chaohu (30°58′–32°06′N/116°24′–118°00′E), which is located in Anhui Province, is the fifth largest freshwater lake in China. It is the primary source of drinking water for the provincial capital city, Hefei and for a medium city, Chaohu. Lake Chaohu covers an area of 753 km^2 and is located in one of the most developed areas in China, the Yangtze River Delta Economic Zone. The local sources of PAHs emission in the Lake Chaohu area are of complexity, due to the effects from the northwest Hefei city and eastern Chaohu City, the southern and northern rural areas, as well as from the lake tourism. The primary PAHs source in the urban areas is vehicle emission, while that in the rural areas is the combustion of biomass fuels (e.g. straw, firewood). The coal combustion in the nearby power plants is also an important PAHs source. In addition, the long distance transportation from the adjacent provinces is the secondary PAHs sources in Lake Chaohu area.

Some studies have examined the air–water exchange in China (Fang et al., 2008; Qiu et al., 2008, 2010; Li et al., 2009; Devi et al., 2011), but diffusive fluxes vary according to meteorological and geographical conditions (Bidleman, 1999). To understand the atmospheric influence of the Lake Chaohu aquatic system, it is necessary to study the specific pollution characteristics of atmospheric PAHs, identify the partitioning characteristics and to evaluate the exchange fluxes through the air–water interface. The aim of this study included the following: (1) to investigate the residual levels, composition characteristics and seasonal variation of PAHs in atmospheric samples and lake water; (2) to elucidate the partitioning of PAHs in gaseous and particulate phases; and (3) to investigate the uncertainty of estimates of the air–water exchange and the sensitivity of the parameters.

2. Materials and methods

2.1. Sample collection and pretreatment

Atmosphere samples and water samples were collected once a month from May 2010 to April 2011. The sampling sites are shown in Fig. S1 in the Supporting information. High-volume samplers were placed on the roofs of residential buildings on the island and on the Environmental Protection Agency building. Polyurethane foam (PUF) disks and glass fiber filters (GFFs) were used to collect gaseous-phase PAHs and particulate-phase PAHs. The average flow rate was 0.31 $m^3\ min^{-1}$. After sampling, both the PUF and the GFF were packed in aluminum foil and stored at 20 °C. Twenty liters of water was collected from each sampling site. After shaking and mixing, a 1-L aliquot of each collected water sample was filtered through a 0.45-μm glass fiber filter (burned at 450 °C for 4 h) using a filtration device consisting of a peristaltic pump (80EL005, Millipore Co., USA) and a filter plate with a diameter of 142 mm. Surrogate standards of 2-fluoro-1, 1′-biphenyl and p-terphenyl-d14 (J&K Chemical, USA, 2.0 mg mL^{-1}) were added to the water samples to indicate the recovery before extraction.

In the laboratory, the PUF was Soxhlet extracted with a 150 mL 1:1 mixture of n-hexane and acetone for 8 h. The GFF was extracted with a 25 mL hexane/acetone mixture (1:1) using a microwave accelerated reaction system (CEM Corporation, Matthews, NC, USA). The microwave power was set at 1200 W, and the temperature was ramped to 100 °C over 10 min and then held at 100 °C for another 10 min. Both PUF and GFF extracts were concentrated to 1 mL by rotary evaporation at a temperature below 38 °C and then transferred to a silica/alumina chromatograph column for cleanup. The elution solution was collected, concentrated, conversed to hexane solution, and then added with internal standards (Nap-d8?Ace-d10?Ant-d10?Chr-d12 and Perylene-d12, J&K Chemical Ltd., USA).

The water samples were extracted using a solid phase extraction (SPE) system (Supelco). C18 cartridges (500 mg, 6 ml, Supelco) were prewashed with dichloromethane (DCM) and conditioned with methanol and de-ionized water. A 1-L water sample passed through the SPE system and was extracted. The cartridges were eluted with 10 mL of dichloromethane. The volume of the extracts was reduced by a vacuum rotary evaporator (R-201, Shanghai Shen Sheng Technology Co., Ltd., Shanghai, China) in a water bath and was adjusted to a volume of 1 ml with hexane. Internal standards (Nap-d8, Ace-d10, Ant-d10, Chr-d12 and Perylene-d12) were added for the GC analysis.

2.2. Sample analysis and quality control

All samples were analyzed on a GC–MS (Agilent 6890GC/5973MSD). A 30 m × 0.25 mm i.d. with a 0.25-μm film thickness HP-5MS capillary column (Agilent Technology) was used. The column temperature was programmed to increase from 60 °C to 280 °C at 5 °C min^{-1} and was then held constant for 20 min. The MSD was operated in the electron impact mode at 70 eV, and the ion source temperature was 230 °C. The mass spectra were recorded using the selected ion monitoring mode. The concentrations of 16 PAHs were determined: naphthalene (Nap), acenaphthene (Ace), acenaphthylene (Acy), fluorine (Flo), phenanthrene (Phe), anthracene (Ant), fluoranthene (Fla), pyrene (Pyr), benz(a)anthracene (BaA), chrysene (Chr), benzo(b)fluoranthene (BbF), benzo(k)fluoranthene (BkF), benzo(a)pyrene (Bap), dibenz(a, h) anthracene (DahA), indeno(1,2,3-cd)pyrene (IcdP) and benzo(g, h, i) perylene (BghiP).

The quantification was performed by the internal standard method using Nap-d8, Ace-d10, Ant-d10, Chr-d12 and Perylene-d12 (J&K Chemical, Beijing, China). All of the solvents used were HPLC-grade pure (J&K Chemical, Beijing, China). All of the glassware was cleaned using an ultrasonic cleaner (KQ-500B, Kunshan, China) and heated to 400 °C for 6 h. In the sampling process, three replicate samples were collected from each sample site. Laboratory blanks were analyzed with the true samples. The recovery methods and detection limits are shown in Table S1 in the Supporting information. The detection limits were in the range of 0.64–1.85 ng L^{-1}. The PAH recoveries for gaseous phase, particulate phase and water varied from 46% to 124%; 47% to 119% and 21% to 122%, respectively.

Please cite this article in press as: Qin, N., et al. Atmospheric partitioning and the air–water exchange of polycyclic aromatic hydrocarbons in a large shallow Chinese lake (Lake Chaohu). Chemosphere (2013), http://dx.doi.org/10.1016/j.chemosphere.2013.05.038

3. Results and discussion

3.1. PAH residue levels in atmosphere and water samples at Lake Chaohu

In total, 16 PAHs in gas-phase, particulate-phase and water samples from May, 2010 to April, 2011 were analyzed. The PAH residue levels are summarized in Table 1. The concentration of gas-phase PAH16 ranged from 16.49 to 184.63 ng m^{-3} with an average value of 60.85 ± 46.17 ng m^{-3}. Phe had the highest value (24.06 ± 23.88 ng m^{-3}), followed by Fla (14.88 ± 10.39 ng m^{-3}) and Pyr (8.59 ± 4.00 ng m^{-3}). DahA had the lowest concentration of 0.01 ± 0.01 ng m^{-3}. PAH16 was dominated by the low-molecular-weight (LMW) PAH, which accounted for 81.9% of the total PAH16 concentration. Moderate-molecular-weight (MMW) PAH and high-molecular-weight (HMW) PAHs accounted for 17.9% and 0.02% of total PAH16, respectively. A one-way ANOVA was employed to analyze the statistical differences among sampling sites, and no significant differences were observed ($p = 0.195$).

Particulate-phase PAH16 concentrations during the sampling period were in the range of 3.49–75.90 ng m^{-3} with an average value of 14.32 ± 23.82 ng m^{-3}. These values were much lower than the gas-phase PAH16 concentrations. Compared with gas samples, LMW PAHs in particles represented a smaller proportion of the total, 22.7%. MMW and HMW PAHs contributed 49.9% and 27.4%, respectively, of the total particulate-phase PAH16. Bbf had the highest residual level in particle phase (2.58 ± 4.10 ng m^{-3}), followed by IcdP (1.51 ± 2.47 ng m^{-3}). Acy had the lowest concentration of 0.02 ± 0.04 ng m^{-3}. No significant statistical differences were observed between the two sampling sites (one-way ANOVA, $p = 0.981$).

The hydrophilicity of PAHs decreases with increasing molecular weight, and thus, the detection rates of PAHs followed the order HMW < MMW < LMW in water samples. LMW PAHs were 100% detected. Two kinds of MMW PAHs (Bbf, Bkf) were 50% detected. The detection rates for HMW PAHs were as follows: Bap (25.0%), IcdP (16.7%), DahA (8.3%) and BghiP (16.7%). The concentration ranged from 69.92 to 515.62 ng L^{-1} with a mean of 173.46 ± 132.89 ng L^{-1}. Because of the low detection of MMW and HMW PAHs, the contribution of the LMW PAHs was dominant, at 92.9%, and MMW and HMW accounted for only 7% and 0.08% of the dissolved PAHs, respectively. Statistical analysis was applied to test for differences among the three sampling sites, and no significant difference was found (one-way ANOVA, $p = 0.989$).

The atmospheric residual levels (particulate + gas) of PAHs in Chaohu (60.85 ng m^{-3} + 14.32 ng m^{-3}) were significantly lower than the 313 ng m^{-3} + 23.7 ng m^{-3} reported for Guangzhou (Li et al., 2006), which belongs to the Pearl River Delta Economic Development Zone in southern China and is lower than that of Tianjin (485 ng m^{-3} + 267 ng m^{-3}), which belongs to the Beijing–Tianjin–Tangshan Economic Development Zone in eastern China (Liu et al., 2008). These comparisons showed that the PAH residual levels in the atmospheric samples in this study were lower than those found in the previous studies in big Chinese cites, which may be attributed to the difference in the economic development levels and population sizes. It was reported that the atmospheric emission of PAHs was positively correlated to the local gross domestic product (GDP) and population (Zhang and Tao, 2009). The population in Hefei (4.5 million) was much lower than that in the big Chinese cities such as Beijing (20 million), Guangzhou (17 million) and Tianjin (10 million); and the GDP in 2011 in Hefei City (270.250 billion Chinese Yuan (RMB)) was also much lower than that in Beijing (1377.790 billion RMB), Guangzhou (1060.448 billion RMB) and Tianjin (910.883 billion RMB).

Compared with studies outside of China, the results in the present study were comparable to the levels reported in Izmir, Turkey (PAH15 average 25.2–44.1 ng m^{-3} in winter) (Demircioglu et al., 2011), in the Southern Chesapeake Bay (total 5.3–71.6 ng m^{-3}) (Gustafson and Dickhut, 1997b) and in Athens, Greece (4.8–76 ng m^{-3}) (Mandalakis et al., 2002). The concentrations in Lake Chaohu were also lower than those reported for samples from Lake Michigan near Chicago (PAH14, 92.3–244.9 ng m^{-3}) (Vardar et al., 2004). The concentration of dissolved-phase ∑PAH16 in Lake Chaohu (173.46 ± 132.89 ng L^{-1})was a bit higher than that reported in Lake Taihu (134.5 ± 54.8 ng L^{-1}) (Qiao et al., 2008), but much lower than the levels in Lake Victoria (3.32–55.8 μg L^{-1}) (Kwach and Lalah, 2009).

Table 1
Contents of PAHs in air and water.

	Gaseous phase (ng m^{-3})			Particulate phase (ng m^{-3})			Dissolved phase (ng L^{-1})		
	Range	GM	SD	Range	GM	SD	Range	GM	SD
Nap	0.27–4.53	1.36	1.40	0.06–0.31	0.18	0.08	27.28–145.83	58.04	30.91
Acy	0.05–5.14	0.75	1.70	0.00–0.12	0.02	0.04	2.04–48.66	7.17	17.35
Ace	0.12–1.25	0.40	0.39	0.01–0.08	0.04	0.02	7.16–153.42	22.50	49.26
Flo	1.10–17.22	4.54	5.28	0.04–0.36	0.14	0.12	8.07–75.41	20.02	19.40
Phe	5.86–88.95	24.06	23.88	0.20–4.40	0.89	1.33	7.13–128.40	29.36	33.69
Ant	0.19–9.81	1.86	2.51	0.04–0.23	0.10	0.07	0.82–9.75	3.39	2.67
Fla	3.70–39.94	14.88	10.39	0.39–8.79	1.39	2.89	1.74–11.50	5.61	2.95
Pyr	3.72–17.82	8.59	4.00	0.31–10.25	1.43	3.60	3.13–19.71	5.99	4.65
Baa	0.09–0.59	0.33	0.15	0.13–6.01	0.67	1.92	0.33–2.42	1.09	0.67
Chr	0.37–1.76	1.07	0.39	0.20–10.97	1.27	3.63	0.39–4.73	1.72	1.22
Bbf	0.02–0.54	0.20	0.16	0.65–13.70	2.58	4.10	ND–1.45	0.81	0.54
Bkf	0.02–0.41	0.12	0.10	0.24–4.41	0.92	1.25	ND–2.15	0.73	0.67
Bap	ND–0.25	0.05	0.07	0.20–5.22	0.86	1.57	ND–0.92	0.22	0.26
IcdP	ND–0.23	0.02	0.07	0.40–8.51	1.51	2.47	ND–0.34	0.13	0.10
DahA	ND–0.03	0.01	0.01	0.05–0.99	0.18	0.30	ND–0.06	0.06	0.02
BghiP	ND–0.26	0.02	0.08	0.46–5.59	1.39	1.52	ND–0.52	0.48	0.19
LMW	12.14–166.84	49.10	44.06	0.79–14.17	2.91	4.42	59.82–491.07	161.00	129.83
MMW	4.35–19.28	10.50	4.24	1.58–43.34	7.17	13.93	5.28–24.54	10.13	5.57
HMW	0–0.77	0.08	0.21	1.12–20.32	3.99	5.82	0–1.42	0.46	0.49
PAH16	16.49–184.63	60.85	46.71	3.49–75.90	14.32	23.82	69.92–515.62	173.46	132.89

GM: Geometric mean; SD: standard deviation.
PAH16: the sum of 16 PAH components; LMW-PAH: low-molecular-weight PAHs including 2–3-ring PAHs (Nap, Acy, Ace, Flo, Phe, Ant, Fla); MMW-PAH: moderate-molecular-weight PAHs including 4-ring PAHs (Pyr, Baa, Chr, Bbf, Bkf); HMW-PAH: high-molecular-weight PAHs including 5–6-ring PAHs (Bap, IcdP, DahA, BghiP).

Please cite this article in press as: Qin, N., et al. Atmospheric partitioning and the air–water exchange of polycyclic aromatic hydrocarbons in a large shallow Chinese lake (Lake Chaohu). Chemosphere (2013), http://dx.doi.org/10.1016/j.chemosphere.2013.05.038

3.2. Seasonal variation of PAH levels

The PAH16 concentrations for different seasons and in various air temperatures are illustrated in Fig. 1. The average concentrations of PAH16 in the gaseous phase for each season were ordered as follows: winter (137.47 ± 41.69 ng m^{-3}) > autumn (65.80 ± 10.12 ng m^{-3}) > summer (47.62 ± 20.94 ng m^{-3}) > spring (43.09 ± 33.20 ng m^{-3}). The values for particulate samples according to season were the following: winter (56.13 ± 22.99 ng m^{-3}) > spring (19.02 ± 12.14 ng m^{-3}) > autumn (11.89 ± 13.48 ng m^{-3}) > summer (6.62 ± 2.72 ng m^{-3}). The PAH16 residual levels in dissolved samples also varied by season as follows: summer (360.00 ± 176.60 ng L^{-1}) > autumn (174.33 ± 104.13 ng L^{-1}) > spring (142.73 ± 20.70 ng L^{-1}) > winter (142.68 ± 74.68 ng L^{-1}). The PAHs in the gaseous and particulate phases followed similar seasonal trends with regard to temperature; however, the trend in water samples was different. The monthly averaged temperature in Chaohu ranged from 272.6 K (January) to 301.8 K (August). The highest concentration of gaseous- and particulate-phase PAHs were both in winter samples; the values were 184.63 ng m^{-3} for the gaseous and 75.90 ng m^{-3} for the particulate phase in December. The lowest levels were 16.49 ng m^{-3} (April) and 3.50 ng m^{-3} (August). The highest level for the dissolved phase was 396.33 ng L^{-1} in July, and the lowest level was 69.92 ng L^{-1} in November.

Correlation analysis was applied to test the relationship between temperature and PAH16 concentrations in different media. A positive correlation ($p < 0.05$) was found between temperature and dissolved PAH content, whereas there was a negative correlation between temperature and PAH concentration in the gas-phase ($p < 0.05$) and particulate-phase samples ($p < 0.01$). The results of the correlation analysis suggest that temperature was an important factor in determining the PAH levels in both the atmosphere and in bodies of water. It can be found from the Fig. 1 that, the temperature observed on January was the lowest; however, the content of the aquatic PAHs was higher than December and February. It was mainly due to the impact of atmospheric deposition. Meteorological data showed that, a total of 7.6 mm snow precipitation was found during the sampling period in January 2011. This atmospheric deposition might have a significant influence on the PAHs contents in water. Atmospheric particulate PAHs entered the water system in the form of wet deposition, which might increase the dissolved PAHs concentration through the repartition between water and suspended particle materials.

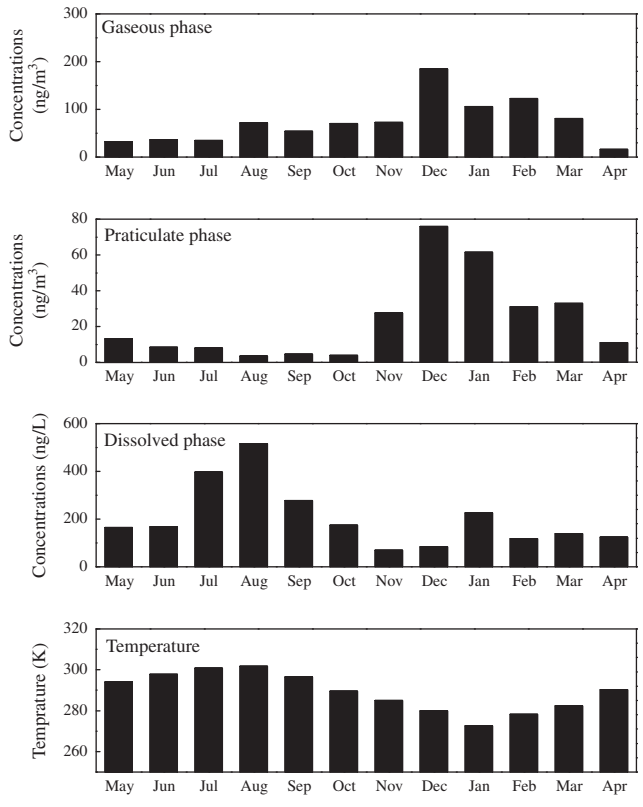

Fig. 1. Average monthly temperature and PAH16 levels in atmospheric and water samples from Lake Chaohu.

3.3. Gas-particle partitioning

The partitioning of PAHs between vapor and solid phase can be described by both the particle-gas partition ratio (P/G) and the gas-particle partition coefficient (K_p) (Simcik et al., 1998; Odabasi et al., 2006; Ma et al., 2011). The following Eqs. (1) and (2) were used to calculate the P/G and K_p of PAHs:

$$P/G = \frac{C_{particle}}{C_{gas}} \quad (1)$$

$$K_p = \frac{C_{particle}}{C_{gas}TSP} \quad (2)$$

where $C_{particle}$ (ng m^{-3}) and C_{gas} (ng m^{-3}) are the PAHs concentrations in the particle phase and in the gas phase, respectively. TSP (μg m^{-3}) is the total suspended particulate concentration. P/G and K_p are the particle-gas partition ratio and the gas-particle partition coefficient, respectively.

The statistical characteristics and the temporal–spatial variations of PAHs' P/G in Lake Chaohu are presented in Table S2 and Fig. S2, respectively. The geometric mean of PAHs' P/G ranged from 0.03 ± 0.15 (Flo) to 159.66 ± 294.96 (IcdP), with the average value of 0.24 ± 0.33. The geometric mean of P/G ratios for the LMW, MMW and HMW PAHs were 0.07, 6.01 and 88.56, respectively. This indicates that the P/G ratios are increased with the increase of molecular weight of PAHs, and that the HMW PAHs are more easily distributed in the particulate phase. It can be seen from Fig. S2 that, during May–December 2010, the P/G ratios of PAH16 were with very similar values and variation trends. From May to August 2010, the P/G ratios had a decreasing trend; however, from August to December 2010, the P/G ratios had an increasing trend.

The gas-particle partitioning of PAHs might be influenced by the weather condition and the TSP content. The relationships between the P/G ratios of PAHs and the ambient air temperature and humidity as well as TSP concentrations in the sampling period were presented in Table S3. The significant negative correlations were found between the P/G ratios of PAH16 and the air temperature at the site HB ($R = -0.631$, $p < 0.05$), and between the P/G ratios and the air humidity at the site MS ($R = -0.650$, $p < 0.05$); while The significant positive correlations were found between the P/G ratios and the TSP concentrations at both sites HB and MS ($R = 0.597$ and 0.606, $p < 0.05$). There were significant correlations between the P/G ratios of medium molecular weight PAHs and the ambient air temperature and humidity as well as TSP concentrations. This is largely determined by the physical and chemical properties of PAHs. The low molecular weight PAHs with lower boiling point mainly present in the gaseous phase, and easily volatilize from the solid phase; while the high molecular weight PAHs are primarily enriched in particulate phase, and are hardly desorpted from particulate phase. However, the medium molecular weight PAHs can easily be influenced by weather condition, and re-partition between the particulate phase and the gaseous phase.

The statistical characteristics of particulate-gas partition coefficients (K_p) of PAHs in Lake Chaohu are presented in Table S4. The

Please cite this article in press as: Qin, N., et al. Atmospheric partitioning and the air–water exchange of polycyclic aromatic hydrocarbons in a large shallow Chinese lake (Lake Chaohu). Chemosphere (2013), http://dx.doi.org/10.1016/j.chemosphere.2013.05.038

geometric mean of PAHs' P/G ranged from 0.0003 (Acy, Flo, Phe) to 1.165 ± 0.174 (IcdP), with the average value of 0.002 ± 0.0018. The K_p geometric mean for the LMW, MMW and HMW PAHs were 0.00059, 0.0456 and 0.7932, respectively. This means that the K_p values are increased with the increase of molecular weight of PAHs, which is in accordance with the results from the P/G.

In order to explain the partition coefficients, two proposed models for the partitioning mechanism, the sub-cooled liquid vapor pressure based model and the octanol–air partition coefficient-based model (Odabasi et al., 2006) were applied in the present study. Their s model equations are as follows:

$$\log K_p = m_r \log P_L^O + b_r \tag{3}$$

$$\log K_p = m \log K_{oa} + b \tag{4}$$

where $\log P_L^O$ is the sub-cooled liquid vapor pressure; m_r and m are the slope constants; b_r and b are the intercept constants; and K_{oa} is the octanol–air partition coefficient.

Correlation analysis and linear regression were used to detect the relationship between gas-particle partition coefficients of PAHs (K_p) and K_{oa} and P_L^O, as shown in Fig. 2. The significant positive correlation was found between K_p and K_{oa} ($p < 0.01$); and the significant negative correlation was observed between K_p and P_L^O ($p < 0.01$). The relationships can be summarized as follows:

$$\log K_p = 0.35 \log K_{oa} - 7.68 \tag{5}$$

$$\log K_p = -0.34 \log P_L^O - 3.46 \tag{6}$$

The results suggested that K_{oa} and P_L^O values have a significant influence on the partitioning of PAHs between the gas and particle phases. PAHs with higher K_{oa} but lower P_L^O values are more easily absorbed onto particles.

3.4. Air–water exchange

3.4.1. Two-film transport model

The two-film transport model was applied to calculate fluxes of semi-volatile organic contaminants (Whitman, 1923). The overall flux is defined by

$$F = K_{ol}(C_{diss} - \frac{C_{gas}}{H'}) \tag{7}$$

where F is the overall mass flux (ng m^{-2} d^{-1}) and K_{ol} (m d^{-1}) is the overall mass transfer coefficient. ($C_{diss} - C_{gas}/H'$) describes the concentration gradient (ng m^{-3}), and C_{diss} and C_{gas} are the dissolved phase concentration of the compound in water (ng m^{-3}) and the gas phase concentration of the compound in air (ng m^{-3}), respectively. The H' value is calculated as H/RT, where H is the temperature and salinity-corrected Henry's law constant (Pa m^{-3} mol^{-1}), R is the universal gas constant (8.314 Pa m^{-3} K^{-1} mol^{-1}), and T is the absolute temperature at the air–water interface (K).

Eq. (8) was applied to estimate the temperature-corrected H values for PAHs:

$$\ln H_T = \ln H_{298} + 26.39 - 7868/T \tag{8}$$

where H_T and H_{298} are the Henry's Law constants at temperature T and 298 K, respectively.

The overall mass transfer coefficient K_{ol} is defined as

$$\frac{1}{K_{ol}} = \frac{1}{K_{water}} + \frac{1}{K_{air}H'} \tag{9}$$

where K_{water} and K_{air} are the mass transfer coefficients through stagnant layers of water and air (m d^{-1}), respectively.

The mass transfer coefficient for PAHs through the air layers was estimated by

$$K_{A,PAH} = K_{A,H2O}[D_{A,PAH}/D_{A,H2O}]^{0.61} \tag{10}$$

where $K_{A,H2O}$ is the mass transfer coefficient of water through the air layers and $D_{A,PAH}$ and $D_{A,H2O}$ are diffusive coefficients for PAHs and H_2O in the water, respectively. $K_{A,\ H20}$ was estimated by

$$K_{A,H2O} = 0.2U_{10} + 0.3 \tag{11}$$

where U_{10} is the wind speed in m s^{-1} at 10 m.

$K_{W,PAH}$ was estimated by

$$K_{W,PAH} = K_{W,CO2}[S_{C,PAH}/S_{C,CO2}]^{-0.5} \tag{12}$$

where $K_{W,CO2}$ is the mass transfer coefficient for CO_2 across the water layers and $S_{C,PAH}$ and $S_{C,CO2}$ are the Schmidt numbers of the PAHs and CO_2, respectively.

$K_{W,CO2}$ was calculated by:

$$K_{W,CO2} = 0.45U_{10}^{1.64} \tag{13}$$

The Schmidt numbers and diffusive coefficients used in this study are temperature corrected.

3.4.2. Air–water exchange fluxes

The fluxes of PAH16 in the air–water interface at Chaohu were calculated, and monthly PAH16 fluxes and temperature are shown in Fig. 3A and B. Negative values for the flux indicate that PAH absorption into the water column was the dominant exchange process. The diffusive air–water exchange flux of total PAH16 ranged from -1.77×10^4 ng m^{-2} d^{-1} to 1.11×10^5 ng m^{-2} d^{-1} with an average value of 3.45×10^4 ng m^{-2} d^{-1}. The highest positive value was observed in August (1.11×10^5 ng m^{-2} d^{-1}) and followed by that in July (8.67×10^4 ng m^{-2} d^{-1}) and September (6.71×10^4 ng m^{-2} d^{-1}). The greatest negative flux was observed in December (-1.77×10^4 ng m^{-2} d^{-1}) and followed by that in November (-3.62×10^3 ng m^{-2} d^{-1}). The PAH16 flux for the entire year was

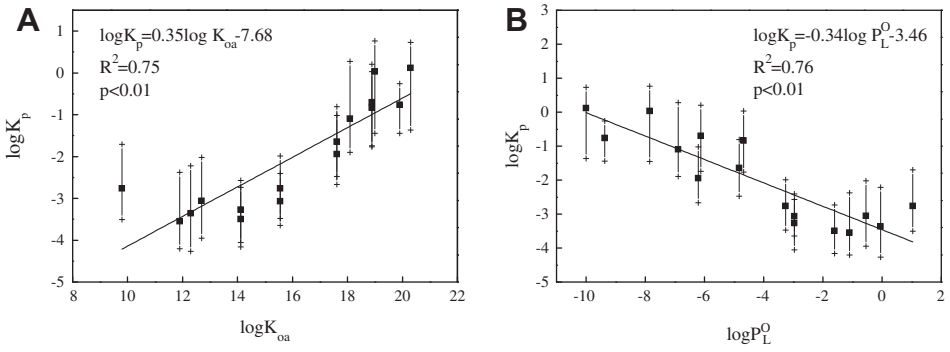

Fig. 2. Regressions of $\log K_p$ versus $\log K_{oa}$ (A) and $\log P_L^O$ (B) for atmospheric PAHs in Lake Chaohu.

Please cite this article in press as: Qin, N., et al. Atmospheric partitioning and the air–water exchange of polycyclic aromatic hydrocarbons in a large shallow Chinese lake (Lake Chaohu). Chemosphere (2013), http://dx.doi.org/10.1016/j.chemosphere.2013.05.038

4.18×10^5 ng m^{-2} d^{-1}. From Fig. 3A, we can also see that the PAH16 flux and temperature have the same trend and that the PAH16 flux has a close relationship with the variation of temperature. Correlation analysis was applied, and the result is shown in Fig. 3. PAH16 fluxes and temperature were significantly correlated (Pearson, $p < 0.01$). Therefore, the air–water exchange of PAHs was usually negative in winter (November and December) or small positive flux (February) owing to the low temperature. However, it can be found from Fig. 3 that January with the lowest temperature had a positive flux from water to air. This might be attributed to the following two reasons. First, the PAHs concentration in the water in January was much higher than that in November and December, due to wet deposition. High PAHs content in the water might cause the positive diffusive exchange flux from the water to the atmosphere. Second, the LMW PAHs in January accounted for 97.3% of total PAHs, which was much higher than the percentages of LMW PAHs in December (88.2%) and November (93.8%). The LMW PAHs are more easily volatilized from the water. From the above analysis, it can be seen that the contents and composition of PAHs in the water and air, as well as the temperature have their impact on the flux direction and value of air–water exchange. The influences of different parameters on the air–water exchange flux were discussed in the Section 3.4.3 "Uncertainty and sensitivity analysis".

The exchange fluxes of the 16 individual PAHs are illustrated in Fig. 4. The differences among the PAH compounds were very large. The annual PAH flux varied from -4.80×10^4 (Fla) ng m^{-2} d^{-1} to 2.36×10^5 (Nap) ng m^{-2} d^{-1} with a mean of 2.59×10^4 ng m^{-2} d^{-1}. Nap had the highest positive flux from water to atmosphere, followed by Ace with the value of 1.44×10^5 ng m^{-2} d^{-1}, and Fla had the greatest negative flux, followed by Pyr with a value of 2.01×10^5 ng m^{-2} d^{-1}. Gustafson and Dickhut (Gustafson and Dickhut, 1997a) found that fluxes of the volatile two-ring PAHs were always from surface waters into the atmosphere, while fluxes of the heavier more non-volatile five-ring PAHs were always from the atmosphere into surface water. A similar conclusion was obtained in this study. The LMW PAHs Nap, Acy, Ace, and Flo have a positive flux from water into the air, but the MMW PAHs and HMW PAHs have a negative flux.

For four important PAHs, the fluxes of the diffusive gas exchange across the air–water interface were compared to values for the Chesapeake Bay in the US and for Lake Luhu in Guangdong, China. The results are shown in Table S5 in the Supporting information.

Fla and Pyr had negative fluxes in all of the studies, but the fluxes documented in China were much higher than those in Chesapeake Bay. This may be attributed to the difference between freshwater and sea water. Flo and Phe in our study had positive average fluxes, whereas they had negative fluxes in the Chesapeake Bay study. The data from Lake Luhu had the most negative values for each of the PAHs, which indicates that the PAHs were moving from air into the water for the entire year.

3.4.3. Uncertainty and sensitivity analysis

The air–water exchange flux was calculated based on monitoring data and the theory of the two-film transport model. However, there is great uncertainty in the monitoring data and in the process of calculating the model. The uncertainty in monitoring data might be mainly from the sampling and analytical errors. It was found that there were some sampling artifacts for the filter-adsorbent samplers in the gas-particle partition of many compounds such as n-alkanes, PAHs, OCPs, PCBs, PFCAs (Cotham and Bidleman, 1992; Simcik et al., 1998; Ahrens et al., 2012). The PAHs exchange between the gaseous and particulate phases could cause both positive and negative sampling artifacts (Hart and Pankow, 1994). Sampling bias caused by the volatilization from the particles is usually referred as the negative particulate-phase artifacts, and the bias caused by the vapor-phase molecule adsorption on the filter or on the collected particles is usually referred as positive particulate-phase artifact (Hart and Pankow, 1994). In addition, the other possible bias can be caused by reaction of NO_2, nitrous acid with several PAHs (Sanderson and Farant, 2005). Some methods have been reported to solve the artifacts. The extent of gas adsorption is often assessed using a second filter method. New sampling systems, for instance diffusion denuders (Tsapakis and Stephanou, 2003; Ahrens et al., 2011) were also developed to avoid the sampling artifacts. However, the filter-adsorbent samplers were employed without artifacts correction in our research, based on the following two reasons. (1) Some previous studies showed that the sampling artifacts had little influence on PAHs gas-particle partition (e.g. Krieger and Hites, 1994; Goss and Schwarzenbach, 1998; Simcik et al., 1998). Simcik and his colleagues used back-up filter and PUF to correct the artifacts of gas absorption, and the results showed that the greatest change in K_p for the PAHs caused by gas absorption was lower than 0.5 log units (Simcik et al., 1998). Goss and Schwarzenbach also suggested that the artifacts in PAHs gas-particle partition caused by gas absorption could be negligible (Goss and Schwarzenbach, 1998). The comparison of the high-volume samplers and the diffusion denuders found that there were no significant sampling artifacts (Krieger and Hites, 1994). (2) During last decades, the development on the diffusive denuders were widely investigated and reported, and the great progress has been made in minimizing the atmosphere particle sampling artifacts of many chemicals. However, the filter-adsorbent system sampler is still the most widely used atmosphere sampling method. Most atmospheric PAHs samples were collected by the high volume active sampler equipped with filter-adsorbent system (GFF-PUF). In order to compare with the large number of existing data, the GFF-PUF was selected in the present study.

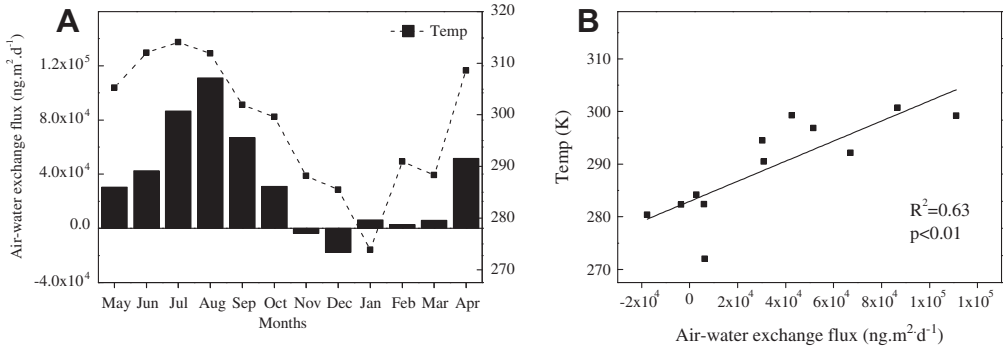

Fig. 3. Net diffusive flux of PAH16 across the air–water interface of Lake Chaohu (A) and correlations between exchange flux and temperature (B).

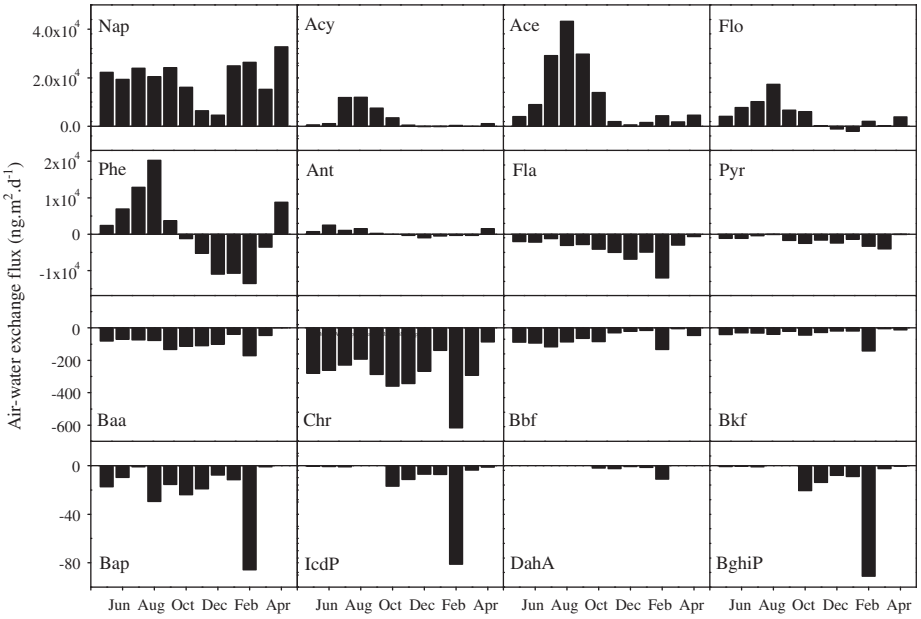

Fig. 4. Air–water exchange and diffusive flux of individual PAHs across the air–water interface in Lake Chaohu.

Model uncertainty may be introduced through the use of empirical and semi-empirical relationships during the research. For example, diffusive coefficients for PAHs in the air were estimated by the semi-empirical relationship proposed by Fuller, and diffusive coefficients for PAHs in the water were estimated by another empirical relationship proposed by Stokes and Einstein and then modified by Hayduk and Laudie.

In this study, a Monte Carlo simulation was run 3000 times to estimate the uncertainties in the calculations of the fluxes. First the Kolmogorov–Smirnov test was applied to the data and to the log-transformed data to test the distribution type, and then, the distribution parameters were calculated. The results are shown in Table S6 in the Supporting information. The distribution parameters *P*1 and *P*2 varied by distribution type. For a normal distribution, *P*1 is the mean value and *P*2 is the standard deviation; for the lognormal distribution, *P*1 is the mean of log-transformed data and *P*2 is the standard deviation of log-transformed data. The concentrations of Bap, IcdP, DahA, and BghiP were not detected in the dissolved phase. They are considered to fit a uniform distribution with the value 0.

The results of the Monte Carlo simulation are shown in Fig. S3 in the Supporting information. The average fluxes (median ± SD) for individual PAHs ranged from $(-3.4 \pm 3.1) \times 10^3$ ng m^{-2} d^{-1} to $(1.6 \pm 1.0) \times 10^4$ ng m^{-2} d^{-1}. Nap has the highest positive flux, and BghiP has the greatest negative flux. Coefficients of variance (CVs) as defined by Eq. (14) are usually used to represent the uncertainty of the fluxes. However, CVs cannot be applied in this research because the fluxes included negative values. Therefore, a modified *CV*′ was applied to measure the uncertainty of the data, as defined in Eq. (15).

$$CV = \frac{\sigma}{\bar{x}} \tag{14}$$

$$CV' = \frac{\sigma}{\max - \min} \tag{15}$$

Among the 16 PAHs, the CVs varied from 0.027 to 0.118. Chr had the highest CV value, followed by Pyr (0.114), DahA (0.11), Nap (0.107), Baa (0.102), Fla (0.090), Bkf (0.084), Flo (0.076), Ace (0.073), Ant (0.060), Bbf (0.051), Acy (0.042), Phe (0.041), IcdP (0.039), and BghiP (0.029). Bap had the lowest value. The result revealed that the Chr flux had the greatest uncertainty. Bap had the lowest uncertainty.

The contributions of the five parameters (concentration in dissolved phase, concentration in gaseous phase, wind speed, temperature and atmospheric pressure) were evaluated by sensitivity analysis, and the results are shown in Fig. S4 in the Supporting information. For Nap, Ace, Acy, Flo, Phe and Ant, the dissolved PAH concentration was the parameter that contributed most of the total variance of the exchange flux. For Nap and Ace, wind speed was the second most important factor affecting the results. Temperature also had an influence on the flux of Nap, likely because Nap and Ace have low molecular weights and low boiling points. Therefore, they are easily affected by the physical parameters of wind speed and temperature. For Flo, Phe and Ant, the gaseous PAH concentration was the second most important factor. For MMW and HMW PAHs (Fla, Pyr, Baa, Chr, Bbf, Bkf, Bap, IcdP, DahA, and BghiP), the value of the air–water exchange flux was predominantly determined by the gaseous concentration because their concentrations were very low in the dissolved phase.

4. Conclusions

This study examined the residual levels and the compositional characteristics of PAHs in the gas and particulate phases and in water samples from Lake Chaohu. The partitioning between gas and particle phases and the factors that influence the partition were also investigated. Finally, diffusive air–water exchange fluxes were estimated by a two-film model, and the flux uncertainty and parameter sensitivity were analyzed. It could be concluded that the PAH16 residual levels in atmospheric samples were lower than those found in previous studies in China. A significant correlation can be observed between temperature and the concentration of PAHs in the three phases. Similarly, significant correlations were established between gas-particle partition coefficients and the sub-cooled liquid vapor pressure and octanol–air partition coefficient. There were large differences in air–water exchange fluxes for different PAHs. LMW PAHs have a positive flux from water to air, but MMW PAH and HMW PAH have a negative flux. Temperature has a significant effect on the flux. The concentration of dis-

Please cite this article in press as: Qin, N., et al. Atmospheric partitioning and the air–water exchange of polycyclic aromatic hydrocarbons in a large shallow Chinese lake (Lake Chaohu). Chemosphere (2013), http://dx.doi.org/10.1016/j.chemosphere.2013.05.038

solved PAHs and the concentration of the gaseous phase PAHS were the two most important factors affecting the calculations.

Acknowledgements

Funding for this study was provided by the National Science Foundation of China (NSFC) (41030529 and 41271462), the National Foundation for the Distinguished Young Scholars (40725004), and the National Project for Water Pollution Control (2012ZX07103-002).

Appendix A. Supplementary material

Supplementary data associated with this article can be found, in the online version, at http://dx.doi.org/10.1016/j.chemosphere.2013.05.038.

References

Ahrens, L., Harner, T., Shoeib, M., Lane, D.A., Murphy, J.G., 2012. Improved characterization of gas-particle partitioning for per- and polyfluoroalkyl substances in the atmosphere using annular diffusion denuder samplers. Environ. Sci. Technol. 46, 7199–7206.

Ahrens, L., Shoeib, M., Harner, T., Lane, D.A., Guo, R., Reiner, E.J., 2011. Comparison of annular diffusion denuder and high volume air samplers for measuring per- and polyfluoroalkyl substances in the atmosphere. Anal. Chem. 83, 9622–9628.

Bidleman, T.F., 1999. Atmospheric transport and air-surface exchange of pesticides. Water Air Soil Pollut. 115, 115–166.

Cotham, W.E., Bidleman, T.F., 1992. Laboratory investigations of the partitioning of organic chlorine compounds between the gas-phase and atmospheric aerosols on glass–fiber filters. Environ. Sci. Technol. 26, 469–478.

Demircioglu, E., Sofuoglu, A., Odabasi, M., 2011. Atmospheric concentrations and phase partitioning of polycyclic aromatic hydrocarbons in Izmir, Turkey. Clean-Soil Air Water 39, 319–327.

Devi, N.L., Qi, S.H., Lv, C.L., Yang, D., Yadav, I.C., 2011. Air–water gas exchange of organochlorine pesticides (OCPs) in Honghu Lake, China. Pol. J. Environ. Stud. 20, 869–875.

Fang, M.D., Ko, F.C., Baker, J.E., Lee, C.L., 2008. Seasonality of diffusive exchange of polychlorinated biphenyls and hexachlorobenzene across the air–sea interface of Kaohsiung Harbor, Taiwan. Sci. Total Environ. 407, 548–565.

Fernandes, M.B., Sicre, M.A., Boireau, A., Tronczynski, J., 1997. Polyaromatic hydrocarbon (PAH) distributions in the Seine River and its estuary. Mar. Pollut. Bull. 34, 857–867.

Franz, T.P., Eisenreich, S.J., Holsen, T.M., 1998. Dry deposition of particulate polychlorinated biphenyls and polycyclic aromatic hydrocarbons to Lake Michigan. Environ. Sci. Technol. 32, 3681–3688.

Goss, K.U., Schwarzenbach, R.P., 1998. Gas/solid and gas/liquid partitioning of organic compounds: critical evaluation of the interpretation of equilibrium constants. Environ. Sci. Technol. 32, 2025–2032.

Gustafson, K.E., Dickhut, R.M., 1997a. Gaseous exchange of polycyclic aromatic hydrocarbons across the air–water interface of southern Chesapeake Bay. Environ. Sci. Technol. 31, 1623–1629.

Gustafson, K.E., Dickhut, R.M., 1997b. Particle/gas concentrations and distributions of PAHs in the atmosphere of southern Chesapeake Bay. Environ. Sci. Technol. 31, 140–147.

Hart, K.M., Pankow, J.F., 1994. High-volume air sampler for particle and gas sampling.2. Use of backup filters to correct for the adsorption of gas-phase polycyclic aromatic hydrocarbons to the front filter. Environ. Sci. Technol. 28, 655–661.

Kavouras, I.G., Koutrakis, P., Tsapakis, M., Lagoudaki, E., Stephanou, E.G., Von Baer, D., Oyola, P., 2001. Source apportionment of urban particulate aliphatic and polynuclear aromatic hydrocarbons (PAHs) using multivariate methods. Environ. Sci. Technol. 35, 2288–2294.

Khalili, N.R., Scheff, P.A., Holsen, T.M., 1995. PAH source fingerprints for coke ovens, diesel and gasoline-engines, highway tunnels, and wood combustion emissions. Atmos. Environ. 29, 533–542.

Krieger, M.S., Hites, R.A., 1994. Measurement of polychlorinated-biphenyls and polycyclic aromatic-hydrocarbons in air with a diffusion denuder. Environ. Sci. Technol. 28, 1129–1133.

Kwach, B.O., Lalah, J.O., 2009. High concentrations of polycyclic aromatic hydrocarbons found in water and sediments of car wash and Kisat Areas of Winam Gulf, Lake Victoria-Kenya. Bull. Environ. Contam. Toxicol. 83, 727–733.

Larsen, R.K., Baker, J.E., 2003. Source apportionment of polycyclic aromatic hydrocarbons in the urban atmosphere: a comparison of three methods. Environ. Sci. Technol. 37, 1873–1881.

Li, J., Cheng, H.R., Zhang, G., Qi, S.H., Li, X.D., 2009. Polycyclic aromatic hydrocarbon (PAH) deposition to and exchange at the air–water interface of Luhu, an urban lake in Guangzhou, China. Environ. Pollut. 157, 273–279.

Li, J., Zhang, G., Li, X.D., Qi, S.H., Liu, G.Q., Peng, X.Z., 2006. Source seasonality of polycyclic aromatic hydrocarbons (PAHs) in a subtropical city, Guangzhou, South China. Sci. Total Environ. 355, 145–155.

Liu, S.Z., Tao, S., Liu, W.X., Dou, H., Liu, Y.N., Zhao, J.Y., Little, M.G., Tian, Z.F., Wang, J.F., Wang, L.G., Gao, Y., 2008. Seasonal and spatial occurrence and distribution of atmospheric polycyclic aromatic hydrocarbons (PAHs) in rural and urban areas of the North Chinese Plain. Environ. Pollut. 156, 651–656.

Lohmann, R., Jurado, E., Dachs, J., Pilson, M.Q., 2006. Oceanic deep water formation as a sink of persistent organic pollutants. Abstr. Papers Am. Chem. Soc. 232, 735–742.

Ma, W.L., Sun, D.Z., Shen, W.G., Yang, M., Qi, H., Liu, L.Y., Shen, J.M., Li, Y.F., 2011. Atmospheric concentrations, sources and gas-particle partitioning of PAHs in Beijing after the 29th Olympic Games. Environ. Pollut. 159, 1794–1801.

Mandalakis, M., Tsapakis, M., Tsoga, A., Stephanou, E.G., 2002. Gas-particle concentrations and distribution of aliphatic hydrocarbons, PAHs, PCBs and PCDD/Fs in the atmosphere of Athens (Greece). Atmos. Environ. 36, 4023–4035.

McConnell, L.L., Cotham, W.E., Bidleman, T.F., 1993. Gas-exchange of hexachlorocyclohexane in the great-lakes. Environ. Sci. Technol. 27, 1304–1311.

Menzie, C.A., Potocki, B.B., Santodonato, J., 1992. Exposure to carcinogenic PAHs in the environment. Environ. Sci. Technol. 26, 1278–1284.

Nelson, E.D., McConnell, L.L., Baker, J.E., 1998. Diffusive exchange of gaseous polycyclic aromatic hydrocarbons and polychlorinated biphenyls across the air–water interlace of the Chesapeake Bay. Environ. Sci. Technol. 32, 912–919.

Odabasi, M., Cetin, E., Sofuoglu, A., 2006. Determination of octanol-air partition coefficients and supercooled liquid vapor pressures of PAHs as a function of temperature: application to gas-particle partitioning in an urban atmosphere. Atmos. Environ. 40, 6615–6625.

Pandit, G.G., Sahu, S.K., Puranik, V., Raj, V.V., 2006. Exchange of polycyclic aromatic hydrocarbons across the air–water interface at the creek adjoining Mumbai harbour, India. Environ. Int. 32, 259–264.

Petry, T., Schmid, P., Schlatter, C., 1996. The use of toxic equivalency factors in assessing occupational and environmental health risk associated with exposure to airborne mixtures of polycyclic aromatic hydrocarbons (PAHs). Chemosphere 32, 639–648.

Qiao, M., Huang, S., Wang, Z., 2008. Partitioning characteristics of PAHs between sediment and water in a shallow lake. J. Soils Sediments 8, 69–73.

Qiu, X.H., Zhu, T., Hu, J.X., 2010. Polybrominated diphenyl ethers (PBDEs) and other flame retardants in the atmosphere and water from Taihu Lake, East China. Chemosphere 80, 1207–1212.

Qiu, X.H., Zhu, T., Wang, F., Hu, J.X., 2008. Air–water gas exchange of organochlorine pesticides in Taihu Lake, China. Environ. Sci. Technol. 42, 1928–1932.

Rogge, W.F., Hildemann, L.M., Mazurek, M.A., Cass, G.R., Simoneit, B.R.T., 1993. Sources of fine organic aerosol. 3. Road dust, tire debris, and organometallic brake lining dust-roads as sources and sinks. Environ. Sci. Technol. 27, 1892–1904.

Sanderson, E.G., Farant, J.P., 2005. Atmospheric size distribution of PAHs: evidence of a high-volume sampling artifact. Environ. Sci. Technol. 39, 7631–7637.

Simcik, M.F., Eisenreich, S.J., Lioy, P.J., 1999. Source apportionment and source/sink relationships of PAHs in the coastal atmosphere of Chicago and Lake Michigan. Atmos. Environ. 33, 5071–5079.

Simcik, M.F., Franz, T.P., Zhang, H.X., Eisenreich, S.J., 1998. Gas-particle partitioning of PCBs and PAHs in the Chicago urban and adjacent coastal atmosphere: states of equilibrium. Environ. Sci. Technol. 32, 251–257.

Simonich, S.L., Hites, R.A., 1995. Organic pollutant accumulation in vegetation. Environ. Sci. Technol. 29, 2905–2914.

Totten, L.A., Brunciak, P.A., Gigliotti, C.L., Dachs, J., Glenn, T.R., Nelson, E.D., Eisenreich, S.J., 2001. Dynamic air–water exchange of polychlorinated biphenyls in the New York – New Jersey Harbor Estuary. Environ. Sci. Technol. 35, 3834–3840.

Tsapakis, M., Apostolaki, M., Eisenreich, S., Stephanou, E.G., 2006. Atmospheric deposition and marine sedimentation fluxes of polycyclic aromatic hydrocarbons in the eastern Mediterranean basin. Environ. Sci. Technol. 40, 4922–4927.

Tsapakis, M., Stephanou, E.G., 2003. Collection of gas and particle semi-volatile organic compounds: use of an oxidant denuder to minimize polycyclic aromatic hydrocarbons degradation during high-volume air sampling. Atmos. Environ. 37, 4935–4944.

Vardar, N., Tasdemir, Y., Odabasi, M., Noll, K.E., 2004. Characterization of atmospheric concentrations and partitioning of PAHs in the Chicago atmosphere. Sci. Total Environ. 327, 163–174.

Wania, F., Axelman, J., Broman, D., 1998. A review of processes involved in the exchange of persistent organic pollutants across the air–sea interface. Environ. Pollut. 102, 3–23.

Whitman, W.G., 1923. The two-film theory of gas absorption. Chem. Metallurg. Eng. 29, 146–148.

Xu, F.L., Wu, W.J., Wang, J.J., Qin, N., Wang, Y., He, Q.S., He, W., Tao, S., 2011. Residual levels and health risk of polycyclic aromatic hydrocarbons in freshwater fishes from Lake Small Bai-Yang-Dian, Northern China. Ecol. Model. 222, 275–286.

Xu, F.L., Qin, N., Zhu, Y., He, W., Kong, X.Z., Boudewijn, M.T., He, Q.S., Wang, Y., Ouyang, H.L., Tao, S., 2013. Multimedia fate modeling of polycyclic aromatic hydrocarbons (PAHs) in Lake Small Baiyangdian, Northern China. Ecol. Modell. 252, 246–257.

Xu, S.S., Liu, W.X., Tao, S., 2006. Emission of polycyclic aromatic hydrocarbons in China. Environ. Sci. Technol. 40, 702–708.

Zhang, G., Li, J., Cheng, H., Li, X., Xu, W., Jones, K.C., 2007a. Distribution of organochlorine pesticides in the northern South China Sea: implications for land outflow and air–sea exchange. Environ. Sci. Technol. 41, 3884–3890.

Zhang, Y.X., Tao, S., Cao, J., Coveney, R.M., 2007b. Emission of polycyclic aromatic hydrocarbons in China by county. Environ. Sci. Technol. 41, 683–687.

Zhang, Y.X., Tao, S., 2009. Global atmospheric emission inventory of polycyclic aromatic hydrocarbons (PAHs) for 2004. Atmos. Environ. 43, 812–819.

Please cite this article in press as: Qin, N., et al. Atmospheric partitioning and the air–water exchange of polycyclic aromatic hydrocarbons in a large shallow Chinese lake (Lake Chaohu). Chemosphere (2013), http://dx.doi.org/10.1016/j.chemosphere.2013.05.038